JOURNAL OF COLLOID AND INTERFACE SCIENCE **196,** 267–277 (1997)
ARTICLE NO. CS975209

Kinetics of Permeate Flux Decline in Crossflow Membrane Filtration of Colloidal Suspensions

Seungkwan Hong,[1] Ron S. Faibish, and Menachem Elimelech[2]

School of Engineering and Applied Science, 5732 Boelter Hall, University of California, Los Angeles, California 90095-1593

Received June 10, 1997; accepted October 1, 1997

A series of well-controlled membrane filtration experiments are performed to systematically investigate the dynamic behavior of permeate flux in crossflow membrane filtration of colloidal suspensions. Results are analyzed by a transient permeate flux model which includes an approximate closed-form analytical expression for the change of permeate flux with time. The model is based on a simplified particle mass balance for the early stages of crossflow filtration before a steady-state flux is attained, and Happel's cell model for the hydraulic resistance of the formed particle cake layer. The filtration experiments demonstrate that permeate flux declines faster with increasing feed particle concentration and transmembrane pressure and with a decrease in the particle size of the suspension. It is also shown that crossflow velocity (shear rate) has no effect on permeate flux at the transient stages of crossflow filtration. Pressure relaxation experiments indicate that the particle cake layer is reversible, implying no irreversible deposition (attachment) of particles onto the membrane surface or the accumulated (retained) particles. The experimental results are shown to be in very good agreement with the theoretical predictions, thus verifying the validity of the model for the transient permeate flux in crossflow filtration and the underlying assumptions in the derivation of the model.

Key Words: **crossflow membrane filtration; colloid filtration; permeate flux decline; transient flux; particle cake layer; concentration polarization; membrane fouling.**

1. INTRODUCTION

Pressure-driven membrane filtration is an important process for separation of colloids and particulate matter from liquid suspensions in many fields of engineering and applied science (1, 2). This separation process is used in such diverse applications as removal of suspended particles and pathogenic microorganisms in water and wastewater treatment, food processing, separation processes in the beverage and cosmetic industries, harvesting of bacterial cells, separation of plasma from whole blood, and dewatering of suspended solids such as mineral slurries. Pressure-driven membrane filtration can operate at either crossflow or dead-end flow configuration. It is generally accepted that separation of colloids and suspended matter in a crossflow mode is advantageous over dead-end operation.

During crossflow membrane filtration, suspended particles are transported to the membrane surface by permeate flow due to the imposed pressure drop. Because of the finite size of colloidal particles, particle concentration on the membrane surface reaches its maximum value after a short period of time, and a cake layer starts to form (3, 4). Cake layer formation in membrane filtration can be viewed as a special case of the more generalized phenomenon of concentration polarization (3). The resulting cake layer on the membrane surface increases the hydraulic resistance to permeate flow and, thus, reduces permeate flow through the membrane. Understanding the mechanisms of permeate flux decline and development of predictive models for the behavior of permeate flux in crossflow membrane filtration are therefore of paramount importance to the design and successful applications of this technology.

Experimental crossflow filtration studies involving colloidal suspensions clearly show that particle flux varies with time once a colloidal suspension is introduced to the filtration system (1, 4, 5–7). Typical flux versus time curves show a relatively rapid flux decline rate at the start of the filtration, followed by a more gradual decrease, until a steady-state (or a pseudo-steady-state) flux is approached. Depending on system variables, the transient stage in crossflow filtration of colloidal suspensions can last from minutes to several hours. In this respect, it is rather surprising that, barring a few exceptions (8), most theoretical efforts were devoted to the development of predictive models for the steady-state flux rather than for the transient stages of crossflow filtration (1–4).

At the present time, it is not clear how system variables, such as particle concentration and size, applied pressure, and crossflow (shear) rate influence the transient behavior of permeate flux. The aim of this paper is to systematically investigate the dynamic behavior of permeate flux in the transient stages of crossflow membrane filtration of colloidal particles before a steady-state flux is attained. Crossflow

[1] Current address: Department of Civil and Environmental Engineering, University of Central Florida, Orlando, FL 32816-2450.

[2] To whom correspondence should be addressed. E-mail: elim@seas.ucla.edu.

0021-9797/97 $25.00

filtration experiments were conducted with two suspensions of spherical, monodisperse silica colloids under well-controlled physical and chemical conditions. A transient permeate flux model is presented based on a simplified particle mass balance for the initial stages of crossflow filtration, and Happel's cell model for the hydraulic resistance of the accumulated particles in the cake layer. Experimental results are compared to theoretical predictions and the effects of feed particle concentration, transmembrane pressure, particle size, and crossflow (shear) rate on the dynamics of permeate flux decline are elaborated and discussed.

2. THEORETICAL

2.1. Pressure Drop and Cake Formation

In pressure-driven crossflow membrane filtration, suspended particles are transported to the membrane surface by the permeate flow and form a concentration polarization (CP) layer. As particle accumulation continues, particle concentration near the membrane surface reaches its maximum value and a particle cake layer forms between the membrane surface and the CP layer. Further transport of particles to the membrane surface results in the growth of the cake layer until a steady state is attained. At steady state, the transport of particles from the bulk to the CP layer (above the cake) by the transverse permeate flow is balanced by the longitudinal transport of particles due to the crossflow (3).

Particle accumulation in the cake layer and in the CP layer above the cake provides an additional resistance to permeate flow and, hence, reduces permeate flux. Resulting pressure drops in the crossflow membrane filtration system can be expressed as

$$\Delta P = \Delta P_m + \Delta P_p + \Delta P_c. \quad [1]$$

Equation [1] states that the applied (transmembrane) pressure drop ΔP is equal to the sum of the pressure drops across the membrane (ΔP_m), the polarization layer (ΔP_p), and the cake layer (ΔP_c).

The pressure drop across the membrane is simply the product of membrane resistance R_m and permeate flux v_w:

$$\Delta P_m = v_w R_m. \quad [2]$$

Note that the membrane resistance R_m (N m^{-3} s) used here is equivalent to μR commonly used in filtration studies to express resistance to solvent flow, with μ being the absolute viscosity and R the intrinsic resistance (m^{-1}).

Because the excess particles in the CP layer are stationary with respect to the membrane in the transverse direction, the pressure drop in the CP layer can be obtained by integration of the frictional drag over the excess particles in the entire CP layer (3, 9). It can be shown, however, that once a cake layer forms, the pressure drop in the CP layer is maintained at a critical value (3):

$$\Delta P_p = \frac{3N_{Fc}kT}{4\pi a_p^3}, \quad [3]$$

where k is the Boltzmann constant, T is the absolute temperature, a_p is the particle radius, and N_{Fc} is the critical filtration number at which the cake layer begins to form. Discussion on the importance of the filtration number in crossflow filtration is given elsewhere (3).

Since the particle concentration in the cake layer is fixed, usually at a value corresponding to random packing, the pressure drop in the cake layer at any location in the membrane channel is related to the frictional drag resulting from the flow of permeate through the dense layer of accumulated particles (3):

$$\Delta P_c = \frac{kT}{D} A_S(\theta_{max}) v_w M_c. \quad [4]$$

Here, kT/D ($=6\pi\mu a_p$) is the frictional drag coefficient, D is the particle diffusion coefficient, $A_S(\theta_{max})$ is a correction function accounting for the effect of neighboring retained particles, and M_c is the total number of particles (per unit area) accumulated in the cake layer. The correction function, A_S, can be evaluated from Happel's cell model (10, 11):

$$A_S = \frac{1 + \frac{2}{3}\theta^5}{1 - \frac{3}{2}\theta + \frac{3}{2}\theta^5 - \theta^6}, \quad [5]$$

where $\theta = (1 - \epsilon)^{1/3}$ is a porosity dependent variable, with ϵ being the porosity of the cake layer of accumulated particles. For maximum random packing of spheres (i.e., $\epsilon = 0.36$ or $\theta_{max} = 0.86$), $A_S(\theta_{max}) = 123.22$. The total number of accumulated particles, M_c, is related to the cake layer thickness δ_c by

$$M_c = \frac{\theta_{max}^3}{\frac{4}{3}\pi a_p^3}\delta_c = \frac{3C_c}{4\pi a_p^3}\delta_c, \quad [6]$$

where C_c is the particle volume fraction in the cake layer. Note that θ_{max}^3 in the above equation is the particle volume fraction of the cake corresponding to maximum random packing.

2.2. Particle Transport and Mass Conservation

Particle transport within the CP layer can be described by the convective diffusion equation:

$$\frac{\partial C}{\partial t} + u\frac{\partial C}{\partial x} + v\frac{\partial C}{\partial y} = D\frac{\partial^2 C}{\partial y^2}, \quad [7]$$

where u and v are the fluid velocities in the longitudinal (x) and transverse (y) directions, respectively, C is the particle concentration, and t is the time. In Eq. [7], axial diffusion is neglected because it is much smaller than the other terms under typical conditions of crossflow filtration. In addition, the accumulated particles in the cake layer are assumed to be immobile, implying that particle transport takes place only in the polarized layer above the cake.

With the boundary conditions,

$$vC - D\frac{\partial C}{\partial y} = 0, \quad C = C_c, \quad v = v_w \quad \text{at } y = \delta_c, \qquad [8a]$$

$$\frac{\partial C}{\partial y} = 0, \quad C = C_0, \quad v = v_w \quad \text{at } y = \delta_c + \delta_p, \qquad [8b]$$

Eq. [7] can be integrated over the entire CP layer to yield (12)

$$\frac{\partial}{\partial t}\int_{\delta_c}^{\delta_c+\delta_p}(C - C_0)dy + (C_c - C_0)\frac{\partial \delta_c}{\partial t} + \frac{\partial}{\partial x}\int_{\delta_c}^{\delta_c+\delta_p} u(C - C_0)dy = v_w C_0. \qquad [9]$$

Here δ_p and δ_c are the thicknesses of the CP and cake layers, respectively, and C_0 is the bulk (feed) particle concentration. The terms in Eq. [9] (from left to right) represent particle accumulation in the CP layer, particle accumulation in the cake layer, particle convection in the CP layer by crossflow, and particle convection into the CP layer by permeate flow, respectively. At steady state, the first two transient terms vanish and Eq. [9] reduces to

$$\int_{\delta_c}^{\delta_c+\delta_p} u(C - C_0)dy = C_0\int_0^x v_w dx. \qquad [10]$$

Equation [10] implies that, at steady state, particle transport from the bulk suspension into the CP layer by permeate flow is balanced by the crossflow transport of excess particles ($C - C_0$) in the longitudinal direction (3).

2.3. Approximate Solution for the Transient Permeate Flux

Solving Eq. [9] requires the use of numerical techniques. This equation, however, can be simplified based on assumptions which are reasonably applicable to typical membrane filtration of colloidal suspensions. First, particle accumulation in the CP layer is assumed to reach steady state in a very short time. It has been shown that, depending on hydrodynamic conditions, a steady state in the CP layer is achieved within a very short period of time (13). Second, it is assumed that the initial permeate flux decline is independent of the longitudinal flow. Several studies (1, 12) have indicated that a dead-end filtration theory provides a good approximation when modeling initial permeate flux decline, implying that, at the initial stages of crossflow filtration, most particles brought to the membrane surface by permeate flow deposit in the cake layer and the longitudinal transport of excess particles by crossflow is negligible. Based on the above two assumptions, the first and third terms in Eq. [9] vanish, and the following simple particle mass balance equation is obtained:

$$(C_c - C_0)\frac{d\delta_c}{dt} = v_w C_0. \qquad [11]$$

In membrane filtration of colloidal suspensions, the pressure drop across the CP layer, ΔP_p, is very small compared to the pressure drop across the cake layer. Hence, Eq. [1] simplifies to

$$\Delta P_c = \Delta P - \Delta P_m = \Delta P - v_w R_m. \qquad [12]$$

Combining Eqs. [4], [6], and [12] results in an expression for the cake layer thickness:

$$\delta_c = \frac{4\pi a_p^3 D}{3C_c kTA_S(\theta_{max})}\left(\frac{\Delta P - v_w R_m}{v_w}\right). \qquad [13]$$

Assuming that membrane resistance does not change with time (i.e., no membrane fouling), differentiation of Eq. [13] with respect to time yields

$$\frac{d\delta_c}{dt} = \frac{4\pi a_p^3 D\Delta P}{3C_c kTA_S(\theta_{max})}\left(\frac{-1}{v_w^2}\right)\frac{dv_w}{dt}. \qquad [14]$$

Substituting Eq. [14] in Eq. [11] results in

$$\frac{dv_w}{dt} = \left[\frac{-3C_c kTA_S(\theta_{max})C_0}{4\pi a_p^3 D\Delta P(C_c - C_0)}\right]v_w^3. \qquad [15]$$

Equation [15] can be converted into a more practical form by integrating it with respect to time:

$$\frac{v_w}{v_0} = \left(1 + \frac{3kTA_S(\theta_{max})C_c C_0\Delta P}{2\pi a_p^3 DR_m^2(C_c - C_0)}t\right)^{-1/2}, \qquad [16]$$

where v_0 ($=\Delta P/R_m$) is the initial permeate flux. Lastly, for dilute colloidal suspensions (i.e., $C_0 \ll C_c$), Eq. [16] simplifies to

$$\frac{v_w}{v_0} = \left(1 + \frac{3kTA_S(\theta_{max})C_0\Delta P}{2\pi a_p^3 DR_m^2}t\right)^{-1/2}. \qquad [17]$$

In the above equations, the bulk (feed) particle concentration

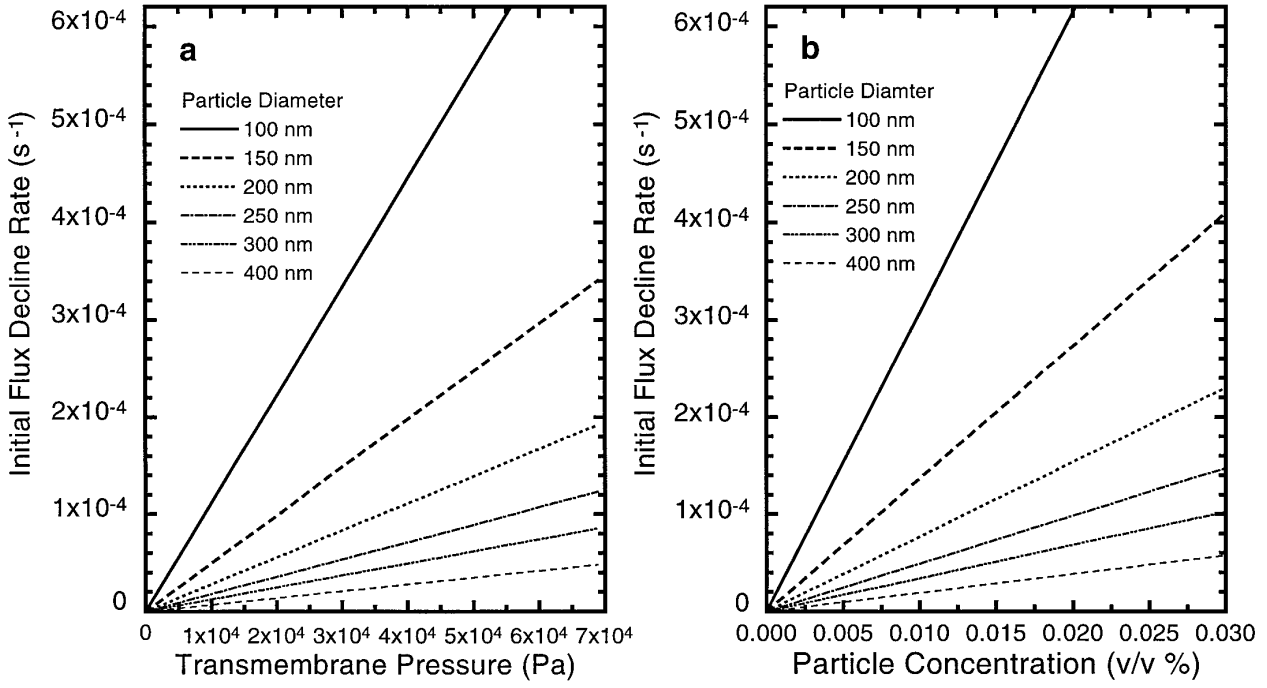

FIG. 1. Theoretical initial permeate flux decline rate (K_0) as a function of (a) transmembrane pressure and (b) particle volume concentration, for crossflow filtration of suspensions with different particle size. In each figure, particle diameter varies from 100 nm (top curve) to 400 nm (bottom curve). The parameters used in the theoretical calculations are: membrane resistance = 1×10^9 N m^{-3} s, temperature = 20°C, porosity = 0.36 (or $\theta = \theta_{max} = 0.86$), particle volume concentration = 0.005% for (a), and transmembrane pressure = 13.8 k Pa for (b).

(C_0) and the cake layer particle concentration (C_c) are given as volume fractions.

2.4. Representative Theoretical Predictions

For the initial stage of membrane filtration, Eq. [17] can be simplified through series expansion to

$$\frac{v_w}{v_0} = 1 - \frac{3kTA_S(\theta_{max})C_0\Delta P}{4\pi a_p^3 D R_m^2}\, t. \qquad [18]$$

This equation is valid when the second term in the brackets of Eq. [17] is much smaller than 1. Differentiation of Eq. [18] with respect to time yields

$$K_0 = -\frac{1}{v_0}\frac{dv_w}{dt} = \frac{3kTA_S(\theta_{max})C_0\Delta P}{4\pi a_p^3 D R_m^2}, \qquad [19]$$

where K_0 is a measure of the initial permeate flux decline rate. When expressed in terms of bulk particle number concentration n_0 rather than particle volume fraction C_0, Eq. [19] is given as

$$K_0 = -\frac{1}{v_0}\frac{dv_w}{dt} = \frac{kTA_S(\theta_{max})n_0\Delta P}{D R_m^2} \qquad [20]$$

Equations [19] and [20] indicate that the initial permeate flux decline rate is a function of the transmembrane pressure, temperature, particle size, feed colloid concentration, and membrane resistance.

Representative theoretical predictions of initial permeate flux decline rates as a function of filtration conditions are shown in Fig. 1. The results demonstrate that the initial flux decline rate increases with transmembrane pressure and particle feed concentration. It is clearly shown that the initial flux decline rate in both cases is much more pronounced for smaller particles. For a given mass (or volume) concentration of particles, the number concentration of smaller particles in the formed cake is greater than that of larger particles, resulting in more resistance to permeate flow and hence greater flux decline. The effect of particle size can be easily seen from Eq. [19]; differentiation of this equation with respect to transmembrane pressure or feed particle volume fraction reveals that the slope of the initial flux decline rate is inversely proportional to the square of the particle radius. In this analysis, the particle diffusion coefficient is related to the particle radius by the well-known Stokes–Einstein equation:

$$D = \frac{kT}{6\pi\mu a_p}, \qquad [21]$$

where μ is the solvent viscosity.

3. EXPERIMENTAL

3.1. Model Colloidal Suspensions

Two suspensions of silica (SiO_2) colloids, denoted as PST-1 and PST-3 by the manufacturer (Nissan Chemicals, Tarrytown, NY), were used as model colloids for the membrane filtration experiments. The particles were received as stable concentrated aqueous suspensions of an alkaline pH. The manufacturer reports that the particles are spherical and have a narrow size distribution. TEM images and dynamic light scattering measurements (Nicomp Model 370, Particle Sizing Systems, Santa Barbara, CA) were used to verify the size, monodispersity, and sphericity of the silica particles. The mean diameters of the PST-1 and PST-3 colloid suspensions determined from TEM images were 100 and 300 nm, respectively. Gravimetric analysis was used to determine the solid content of the silica stock suspensions and the density of the particles. The densities of the 100 and 300 nm silica particles were found to be 2.27 and 2.28 g/cm^3, respectively.

The colloidal stability of the silica suspensions was assessed by monitoring changes in particle size with time using dynamic light scattering. Colloidal stability was determined at pH 10 for three 1:1 electrolyte (KCl) concentrations (10^{-3}, 10^{-2}, and 10^{-1} M). Electrophoretic mobilities of the particles were measured by microelectrophoresis (Lazer Zee Model 501, Pen Kem Inc., Bedford Hills, NY).

3.2. Model Membrane

The membrane selected for the experiments was a zirconia tubular ceramic membrane (Membralox, US Filter Corp., Warrendale, PA), with a reported average pore size of 0.02 μm. The tubular membrane is 250 mm long and 7 mm in diameter. It was housed in a steel membrane case (U.S. Filter Corp., Warrendale, PA). According to the manufacturer, the membrane can operate at a pH range of 0.5 to 13.5 and at temperatures from 4 to 316°C. The water permeability of the membrane at 20°C is reported by the manufacturer to be in the range of $(1.07-1.18) \times 10^{-9}$ m s^{-1} Pa^{-1}.

3.3. Crossflow Membrane Filtration Unit

A schematic diagram of the laboratory-scale, crossflow membrane filtration unit used is shown in Fig. 2. The colloidal suspension was held in a 5-liter polypropylene reservoir and was fed to the inlet port of the membrane module by a peristaltic pump (Cole-Palmer Instrument Co., Niles, IL). The feed flow rate was measured by a flow meter connected to the inlet of the membrane module. Transmembrane pressure was set by a needle valve installed on the outlet side of the membrane module. The transmembrane pressure was measured by a transducer (Model DP15-44, Validyne Engineering Corp., Northridge, CA) connected to the inlet side of the membrane module. The transducer can measure pressures ranging from 0 to 32 psi (220 kPa) with a reported accuracy of ±0.5%. Temperature was controlled at 20°C by circulating chilled water through a stainless-steel coil immersed in water surrounding the container holding the feed suspension. Chilled water was provided by a refrigerated recirculating chiller (Fisher Scientific, Pittsburgh, PA). Permeate flux measurements were done by collecting the permeate at predetermined time intervals in a preweighed beaker and weighing the sample to determine the permeate volume.

3.4. Crossflow Filtration Experiments

Before each experiment, the filtration system was cleaned thoroughly using acidic (pH 3) and basic (pH 11) solutions for 1 h. Both the acidic and basic washes were conducted at zero transmembrane pressure and moderate crossflow rate. The membrane was then conditioned by flowing a particle-free solution having solution chemistry identical to that used in the filtration experiments (i.e., 0.01 M KCl, pH 10) for approximately 1 h to ensure stable performance.

Filtration experiments were performed at various feed particle concentrations, transmembrane pressures, particles sizes, and shear rates. For flux measurements, each permeate sample was collected for a period of 4 min during the first 80 min of the filtration run and for a period of 9 min for the remaining duration of the run. The pH and ionic strength (pH 10 and 0.01 M) of the feed suspensions were adjusted by the addition of NaOH and KCl, respectively. Temperature of feed suspensions during all crossflow experiments was kept at 20°C.

3.5. Pressure–Relaxation Experiments

Pressure–relaxation experiments were conducted to investigate the reversibility of the cake layer. Following 3 h of membrane filtration, the transmembrane pressure was reduced to zero while maintaining crossflow and all other experimental conditions unchanged. After 1 h of crossflow at zero pressure, the transmembrane pressure was set to the value used in the membrane filtration experiment before the pressure relaxation. Flux measurements were then resumed for a period of 60 min.

3.6. Measurement of Deposited Particle Mass

Several experiments were conducted to determine the deposited mass of particles on the membrane surface during crossflow filtration, from which the porosity of the cake layer can be calculated. A feed sample was collected just before the start of the filtration run by a 20 mL volumetric pipette and then every 20 min for the remainder of the run. The UV absorbance of the samples was determined by a UV/vis spectrophotometer (Model 8452A, Hewlett Packard, Palo Alto, CA). Calibration curves for the two silica suspensions showed that the UV absorbance is linearly proportional to the particle mass concentration. The amount of deposited particles was determined from the difference between the initial feed particle concentration and the sample particle concentration.

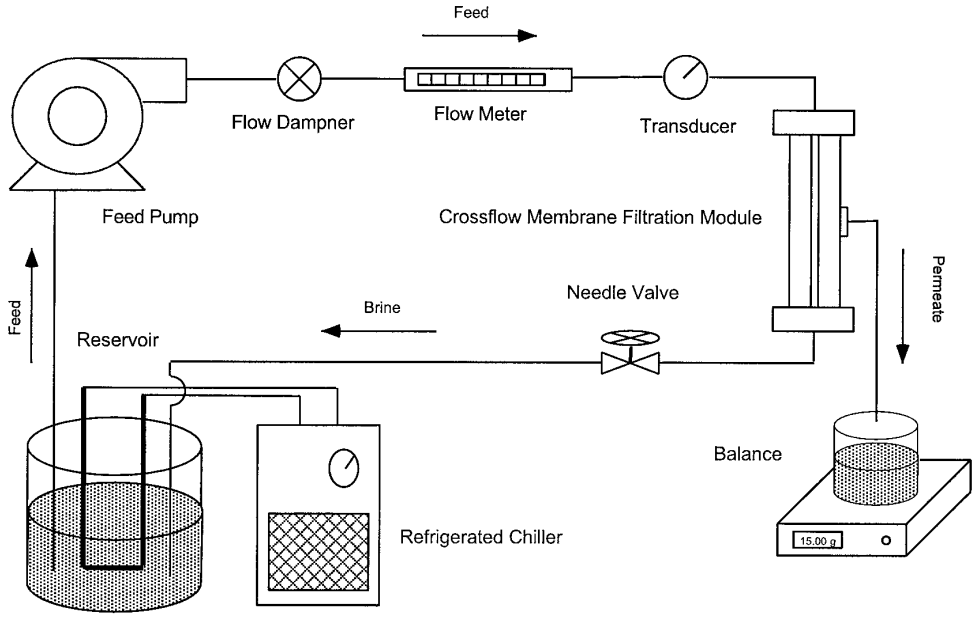

FIG. 2. Schematic description of the laboratory-scale crossflow membrane filtration unit.

4. RESULTS AND DISCUSSION

4.1. Properties of Colloids and Membrane

Particle size and shape are critical in evaluating the dynamic behavior of permeate flux decline because these factors markedly affect particle transport and cake formation. Existing theories and models for particle hydrodynamics in crossflow filtration assume that particles are spherical and monodisperse. The dynamic light scattering measurements and the TEM images showed that the model silica suspensions are monodisperse and that the particles are spherical in shape.

To test the validity of the transient model for crossflow filtration, as well as any other fundamental model for concentration polarization and cake formation, it is imperative that particles do not aggregate prior to deposition on the membrane surface. Furthermore, it is also essential that particles do not attach irreversibly to the membrane surface or to retained particles (a process usually referred to as fouling) during the crossflow filtration experiments. The colloidal stability experiments demonstrated that at pH 10 the two particle suspensions are very stable at the electrolyte concentrations investigated (i.e., 10^{-3}, 10^{-2}, and 10^{-1} M KCl). For particle concentrations typical to those used in the crossflow filtration experiments, no aggregation was detected by dynamic light scattering at 10^{-3} and 10^{-2} M KCl, and a very slow aggregation was observed at 10^{-1} M KCl.

The relatively high stability of the colloidal particles, even at 10^{-1} M KCl, is not surprising since it is rather well known that silica colloids are more stable than other model colloids, such as metal oxides and polymer latex suspensions (14, 15). A recent investigation by Israelachvili and co-workers (15) suggests that the unusual interfacial properties of silica surfaces are attributed to the presence of a thin (ca. 1 nm) gel-like layer of protruding silanol and silicilic acid groups that grow on the surface in the presence of water. The surface gel layer effectively shifts the outer Helmholtz plane outward and adds monotonic short-range repulsion to the electrostatic double layer repulsion.

Based on the above results, it was decided that the crossflow filtration experiments be conducted at an electrolyte concentration of 10^{-2} M KCl and pH 10, where aggregation with the two model colloidal suspensions was not detected by dynamic light scattering. It should be noted that the Debye length at 10^{-2} M KCl is about 3 nm, which is rather small compared to the diameter of the particle suspensions used. Hence, it is not expected that electric double layer repulsion will have a significant effect on the porosity of the cake layers formed during crossflow filtration. Electrophoretic mobility measurements also showed that the particles are highly negatively charged at pH 10 and 0.01 M KCl; the measured electrophoretic mobilities for the 100 and 300 nm silica colloids were -3.0 and -3.1 μm s^{-1} V^{-1} cm, respectively. It is also worthwhile noting that, at pH 10, the zirconia membrane surface is highly negatively charged, since this pH is much higher that the isoelectric point of zirconia which is about 5.8 (16). Hence, it is anticipated that silica colloids will not foul the membrane surface due to the strong electrostatic double layer repulsion between the colloids and the membrane.

Permeability experiments showed that the zirconia membrane has a specific membrane permeability of 0.72×10^{-9} m s^{-1} Pa^{-1} at the tested chemical (pH 10 and 0.01 M KCl) and hydrodynamic (crossflow = 0.246 m/s) conditions. This

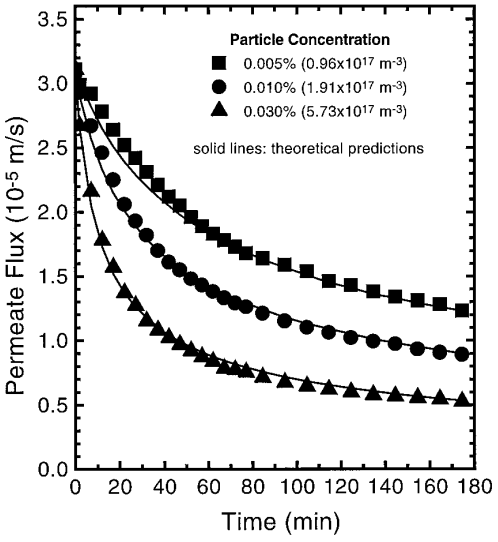

FIG. 3. Effect of particle concentration on permeate flux decline in crossflow filtration with the 100 nm silica suspension. Symbols represent experimental results and solid lines represent theoretical predictions. A porosity of 0.36, corresponding to maximum random packing, was used in the theoretical calculations. Filtration conditions employed were: temperature, 20°C; transmembrane pressure, 41.4 kPa; and shear rate, 280 s^{-1} (or crossflow velocity, 0.246 m/s). The membrane resistance R_m for each run was determined from the initial permeate flux (at $t = 0$) and the transmembrane pressure. Filtration experiments were carried out at pH 10 and 10^{-2} M KCl.

value is slightly smaller than that reported by the manufacturer [$(1.07-1.18) \times 10^{-9}$ m s^{-1} Pa^{-1}]. One hour of membrane conditioning was adequate to achieve a steady-state flux before starting each experimental run. Rejection of small solutes, such as KCl, by the membrane was nearly zero, implying no elevated solute concentration at the membrane surface. Both colloidal suspensions were completely retained by the membranes and no pore blocking was observed.

4.2. *Effect of Particle Concentration*

Figure 3 describes the dynamic behavior of permeate flux decline for three different feed particle concentrations. Each of the filtration experiments was repeated more than twice, and the results were very reproducible. The results demonstrate that permeate flux declines much faster with increasing feed particle concentration. It is also shown that the experimental results are in very good agreement with theoretical predictions based on the model presented earlier in this paper. Theoretical predictions were generated by Eq. [16]; these predictions are practically identical to those obtained from Eq. [17]. A porosity of 0.36, corresponding to maximum random packing (i.e., $C_c = 0.64$ or $\theta = \theta_{max} = 0.86$), was used in the theoretical calculations. Discussion and justification for the use of this value are given in Section 4.7.

The larger decline of permeate flux at higher feed particle concentration is attributed to the increased particle transfer rate to the cake layer. According to the simplified mass balance equation (Eq. [11]), the growth of the cake layer is proportional to the convective particle flux ($v_w C_0$) entering the cake layer. Thus, an increase in feed particle concentration (C_0) enhances particle accumulation in the cake layer, which results in increased hydraulic resistance of the cake layer. The effect of feed particle concentration on the permeate flux can, of course, be seen directly from the derived expression for the permeate flux, Eq. [17].

In addition to increased particle accumulation, there has been some experimental evidence showing the formation of a denser cake layer at higher particle concentrations. Chudacek and Fane (17) demonstrated that the specific resistance of a cake layer composed of silica particles increased with increasing particle concentration. It was suggested that this behavior may result from the increased pressure that accumulated particles at the top of the cake layer exert on the particles in the bottom of the layer. However, the good agreement between the experimental results and theoretical predictions strongly suggests that, under the physical and chemical conditions investigated, the effect of feed particle concentration on the transient permeate flux decline is attributed solely to the increased particle transfer rate as described by Eqs. [11] and [17].

4.3. *Effect of Transmembrane Pressure*

The effect of transmembrane pressure—or alternatively the initial permeate flux v_0 ($=\Delta P/R_m$)—on the permeate flux

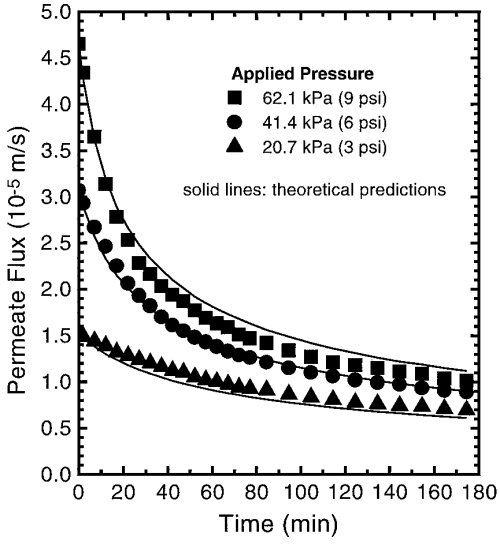

FIG. 4. Effect of transmembrane pressure on permeate flux decline in crossflow filtration with the 100 nm silica suspension. Symbols represent experimental results and solid lines represent theoretical predictions. A porosity of 0.36, corresponding to maximum random packing, was used in the theoretical calculations. Filtration conditions employed were: temperature, 20°C; particle volume concentration, 0.01% (1.91×10^{17} m^{-3}); and shear rate, 280 s^{-1} (or crossflow velocity, 0.246 m/s). The membrane resistance R_m for each run was determined from the initial permeate flux (at $t = 0$) and the transmembrane pressure. Filtration experiments were carried out at pH 10 and 10^{-2} M KCl.

behavior is presented in Fig. 4. The results show that permeate flux declines more rapidly with increasing transmembrane pressure. As with the previous results (Fig. 3), a relatively good agreement is observed between experimental results and theoretical predictions. The behavior shown in Fig. 4 can be explained by the increase in particle deposition rate at higher transmembrane pressures. Particle flux into the cake layer is enhanced at high transmembrane pressures because of the increased permeate flux, causing increased particle accumulation in the cake layer. As time progresses toward steady state, the difference between the permeate fluxes for the three applied pressures decreases. At this stage of the filtration process, the flux behavior is controlled to a large extent by the resistance of the cake layer. Since thicker, and thus more resistant, cake layers are formed at higher applied pressures, the effect of the increased pressure on the permeate flux at the latter stages of the crossflow filtration is not as significant.

Faster flux decline at high transmembrane pressure may also be attributed to the formation of a more densely packed cake layer. It has been experimentally shown that cake layers can be more compressed at high transmembrane pressures due to the drag force induced by permeate flow (17). Consolidation of the particle cake layer by compressive forces results in increased hydraulic resistance of the cake layer and, hence, a lower flux. The rather good agreement between the experimental results and theoretical predictions demonstrated in Fig. 4 points out that such compressive forces (which are not considered in our model) are not significant for the silica cake layer under the conditions investigated, although they may explain the slight deviation between experimental results and theoretical predictions for the run at the highest pressure (62.1 kPa). Compressive forces are important for cake layers formed by deformable colloids (such as proteins) but are probably much less important for rigid, spherical particles as the silica colloids used here.

4.4. *Effect of Particle Size*

The transient permeate flux behavior with the 100 and 300 nm colloidal suspensions under similar physical and chemical conditions is shown in Fig. 5. It is evident that permeate flux declines much faster for the feed suspension with the smaller colloids. Experimental observations are again in very good agreement with theoretical predictions.

As derived earlier (Section 2.4), the rate of initial permeate flux decline is very sensitive to colloid size and increases with decreasing colloid size as $1/a_p^2$, with a_p being the particle radius. Because at the initial (transient) stage of cake formation all particles are transported to the membrane surface (see Eq. [11]), the number of colloidal particles in the cake layer, for a given feed volume (mass) concentration, increases markedly with decreasing colloid size. These particles further provide much more hydraulic resistance to permeate flow than larger particles, thus resulting is sharper flux decline. The dependence of the permeate flux on particle size can also be seen directly from Eqs. [16] or [17].

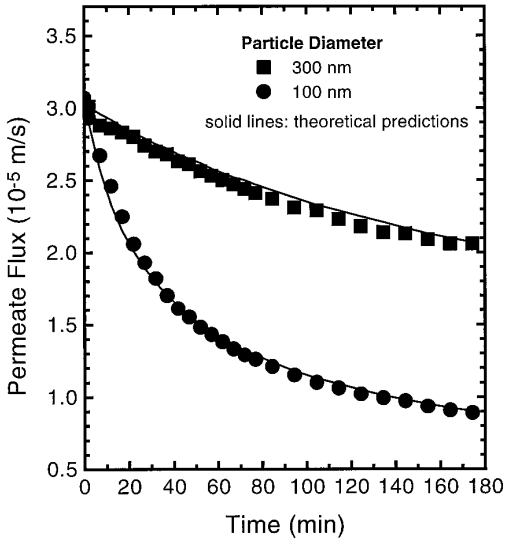

FIG. 5. Effect of particle size on permeate flux decline in crossflow filtration with the two model silica suspensions (100 and 300 nm in diameter). Symbols represent experimental results and solid lines represent theoretical predictions. A porosity of 0.36, corresponding to maximum random packing, was used in the theoretical calculations. Filtration conditions employed were: temperature, 20°C; particle volume concentration, 0.01%; transmembrane pressure, 41.4 k Pa; and shear rate, 280 s^{-1} (or crossflow velocity, 0.246 m/s). The membrane resistance R_m for each run was determined from the initial permeate flux (at $t = 0$) and the transmembrane pressure. Filtration experiments were carried out at pH 10 and 10^{-2} M KCl.

The results in Fig. 5 also demonstrate that, for a given feed mass (or volume) concentration of particles and operational conditions, the approach to steady state is very slow for the larger particles, while it is not too far from steady state for the 100 nm particles after 180 min, under the physical and chemical conditions investigated. The good agreement between theoretical predictions and experimental results for the 100 nm particles also indicates that lateral electrical double layer repulsion between particles in the cake layer did not play an important role in the flux decline behavior. Recent studies point out that the porosity of cake layers comprised of particles smaller than about 100 nm in diameter, can be significantly influenced by the range and magnitude of electrostatic double layer repulsive forces (18, 19). Higher cake porosities, and hence higher permeate fluxes, are expected in membrane filtration of small aqueous colloids at low solution ionic strengths.

Lastly, it should be emphasized that proper accounting for particle accumulation in the cake layer and the hydraulic resistance that the cake layer exerts on the permeate flow is adequate to accurately describe the dynamic (transient) behavior of permeate flux decline in crossflow membrane filtration of colloidal suspensions. In this respect, for a given mass (or volume) feed particle concentration, the size and the resulting number concentration of particles control the hydraulic resistance to permeate flow and, subsequently, the membrane permeate flux. Invoking additional particle transport mechanisms for submicrometer-sized particles, such as

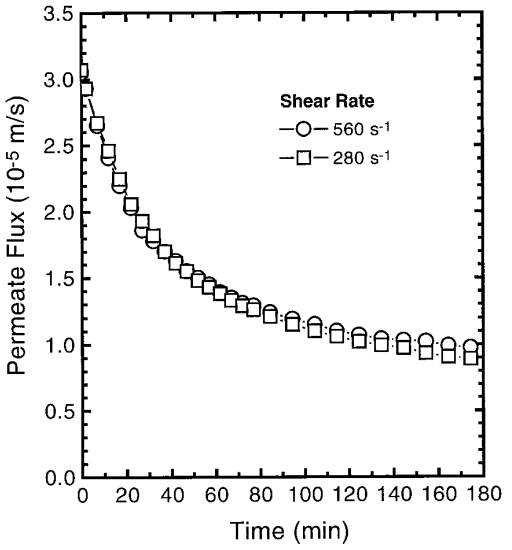

FIG. 6. Effect of shear (crossflow) rate on permeate flux decline in crossflow filtration with the 100 nm silica suspension. Filtration conditions employed were: temperature, 20°C; particle volume concentration, 0.01% (1.91×10^{17} m^{-3}); and transmembrane pressure, 41.4 k Pa. Filtration experiments were carried out at pH 10 and 10^{-2} M KCl.

shear-induced diffusion, may result in erroneous findings in which medium size particles (about 0.5 μm in diameter) attain the steady state flux earlier than smaller particles (8). Our experimental observations, though not long enough to attain the steady-state flux, and the corresponding modeling, do not show such behavior.

4.5. *Effect of Crossflow Velocity*

Figure 6 presents the effect of crossflow velocity (or shear rate) on the transient behavior of permeate flux. Results show that the rate of permeate flux decline at the lower crossflow velocity (0.246 m/s, 280 s^{-1} shear rate) is almost identical to that obtained at the higher crossflow velocity (0.492 m/s, 560 s^{-1}). These results are in accord with theoretical predictions which indicate that, at the initial stages of colloid crossflow filtration, the permeate flux is independent of shear rate. As discussed earlier, during the transient stage of crossflow filtration, all particles are transported to the membrane surface at a rate of $v_w C_0$ (Eq. [11]), and the crossflow velocity has no effect. As the cake layer thickness approaches steady state, the results in Fig. 6 show that the permeate flux increases slightly for the higher shear rate. Theoretical analyses for steady-state crossflow filtration of colloidal suspensions indicate that the permeate flux increases with increasing shear rate, with a flux–shear rate dependence of up to a power of one-third (3).

4.6. *Reversibility of the Polarized Colloid Cake Layer*

Pressure–relaxation experiments were conducted to examine the reversibility of cake layers formed during the crossflow membrane filtration experiments. The dynamic behavior of permeate flux decline before and after relaxing the transmembrane pressure is illustrated in Fig. 7. It is shown that the initial permeate flux is completely recovered after 1 h of pressure relaxation (i.e., under zero transmembrane pressure) while maintaining the usual crossflow (0.246 m/s). This finding suggests that cake formation is reversible and membrane fouling—or irreversible attachment of colloids within the membrane pores or onto the membrane surface—does not occur at the chemical and physical conditions investigated. As soon as the transmembrane pressure is reduced to zero, the accumulated silica colloids diffuse away from the membrane surface due to the concentration gradient which developed during crossflow filtration. Since there is no irreversible particle deposition, all of the silica colloids accumulated in the cake layer are removed from the membrane surface, and, as a result, permeate flux is completely recovered when pressure is applied again.

In addition to complete flux recovery, it is observed that the rate of permeate flux decline after pressure relaxation is identical to that of the original membrane filtration experiment. This result strongly suggests that no aggregation of silica colloids in the cake layer takes place, as indeed observed in our colloidal stability experiments (Section 4.1). During the pressure relaxation stage, particles diffuse away from the membrane surface with no change in their size and, when pressure is re-applied, they accumulate on the membrane surface in a similar fashion as in the run before the pressure relaxation.

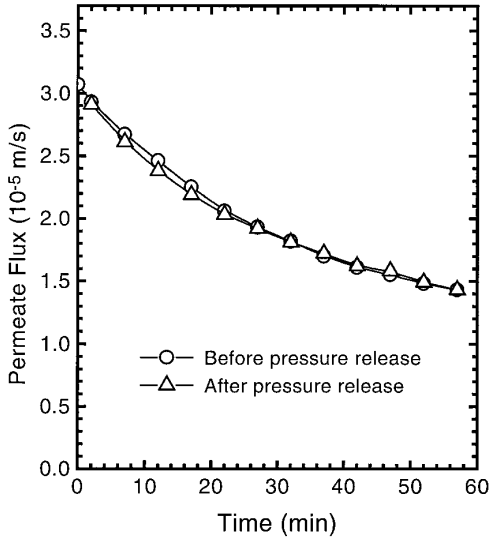

FIG. 7. Permeate flux decline filtration with the 100 nm silica suspension after 1 h of pressure relaxation. Results are compared with filtration data obtained prior to the 1 h pressure relaxation. Filtration conditions employed were: temperature, 20°C; particle volume concentration, 0.01% (1.91×10^{17} m^{-3}); transmembrane pressure, 41.4 k Pa; and shear rate, 280 s^{-1} (or crossflow velocity, 0.246 m/s). Filtration experiments were carried out at pH 10 and 10^{-2} M KCl.

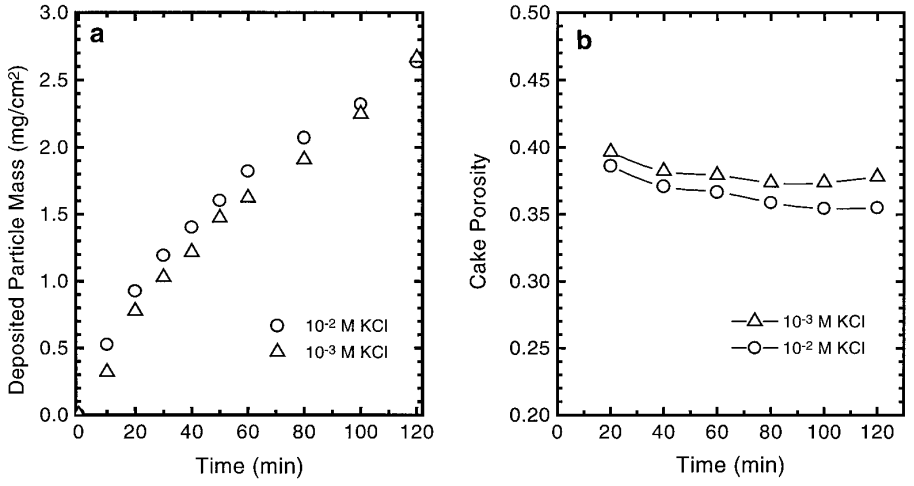

FIG. 8. Change of (a) particle accumulated mass and (b) cake layer porosity for crossflow experiments with the 100 nm particle suspension. Filtration conditions employed were: temperature, 20°C; particle volume concentration, 0.01% (1.91×10^{17} m^{-3}); transmembrane pressure, 41.4 k Pa; and shear rate, 280 s^{-1} (or crossflow velocity, 0.246 m/s). Filtration experiments were carried out at pH 10 and 10^{-2} M KCl.

4.7. On the Choice of Cake Porosity in Crossflow Filtration Modeling

An important parameter in the transient model for crossflow filtration, as well as any other models involving particle cake formation, is the porosity of the accumulated cake layer. In the current model, the porosity is used to calculate the function $A_S(\theta_{max})$ of the Happel cell model (Eq. [5]), with θ_{max} being the value of $\theta = (1 - \epsilon)^{1/3}$ for maximum random packing (or minimum porosity ϵ). We have used a value of $\epsilon = 0.36$ which corresponds to maximum random packing of spherical particles (i.e., $C_c = 0.64$ or $\theta_{max} = 0.86$). Because of the lack of theories or models to unequivocally determine the porosity of cake layers formed during membrane filtration of colloidal suspensions, this value for the cake porosity is commonly used in investigations pertaining to membrane filtration of colloidal suspensions (1–4, 12).

To test whether the choice of a porosity of 0.36 is reasonable, we calculated the porosity from experiments involving measurements of change of the particle deposited mass and the permeate flux with time. By knowing the permeate flux, the deposited mass, the membrane surface area, and the membrane resistance for particle-free solution (R_m), the parameter $A_S(\theta_{max})$ can be calculated, from which the porosity is determined. The results for the particle deposited mass and calculated porosities are shown in Fig. 8 for crossflow experiments with the 100 nm colloid suspension at 10^{-3} and 10^{-2} M KCl. As shown, the porosity of the cake layer is indeed very close to 0.36, thus supporting our choice of that value in the theoretical predictions generated from our transient flux model. The slightly higher values of the porosity at the lower ionic strength (10^{-3} M KCl) are attributable to the lateral electric double layer repulsion between accumulated particles which increases the cake porosity. This important effect, however, is beyond the scope of the present paper, and is a subject of an ongoing investigation. It should also be noted that similar porosities were obtained for the 300 nm particle suspension. The porosities of the cake layers formed with the 300 nm particles at both ionic strengths (i.e., 10^{-3} and 10^{-2} M) were comparable and ranged from 0.35 to 0.37.

5. CONCLUSION

Experimental results and model predictions verify that permeate flux in crossflow membrane filtration of colloidal suspensions declines more rapidly with increasing transmembrane pressure, and when filtering suspensions with higher feed particle concentration and smaller particle size. The transient flux behavior in crossflow filtration of colloidal suspensions is determined by the rate of accumulation of colloidal particles in the cake layer on the membrane surface and the resulting hydraulic resistance that these retained particles exert on the permeate flow. For the most part of the filtration process before a steady permeate flux is attained, the crossflow filtration process is similar to that of dead-end filtration, where the particle accumulation rate on the membrane surface is simply the product of permeate flux and bulk (feed) particle concentration. At the transient stages of the filtration process, crossflow velocity (or shear rate), under laminar flow conditions, has no effect on the permeate flux behavior, and its effect can be seen only before a steady-state permeate flux is attained. The experimental results clearly show that, under chemical conditions in which colloidal stability is maintained, the formation of a cake layer in crossflow filtration is reversible; that is, colloids do not attach irreversibly to the membrane surface or to the accumulated (retained) particles.

APPENDIX: NOMENCLATURE

A_S correction function for the effect of neighboring particles in the cake layer based on Happel's cell model (defined by Eq. [5])
a_p particle radius
C particle volume concentration (fraction)
C_c particle volume fraction of the cake layer
C_0 bulk (feed) particle volume fraction
D particle diffusion coefficient defined by Eq. [21]
K_0 initial permeate flux decline rate defined by Eq. [19]
k Boltzmann's constant (1.38×10^{-23} J K^{-1})
M_c total number of particles (per unit area) accumulated in the cake layer
N_{Fc} critical filtration number at which a cake layer begins to form
n_0 bulk (feed) particle number concentration ($=C_c/(\frac{4}{3}\pi a_p^3)$)
ΔP transmembrane pressure drop (sum of pressure drops across the membrane, cake layer, and CP layer)
ΔP_c pressure drop across the cake layer
ΔP_m pressure drop across the membrane
ΔP_p pressure drop across the concentration polarization layer
R_m membrane hydraulic resistance (units: N m^{-3} s)
T absolute temperature
t time
u longitudinal fluid velocity
v transverse fluid velocity
v_0 initial permeate flux ($=\Delta P/R_m$))
v_w permeate flux
x longitudinal (axial) coordinate (parallel to the membrane surface)
y transverse coordinate (perpendicular to the membrane surface)

Greek Symbols

δ_c thickness of the particle cake layer
δ_p thickness of the concentration polarization layer
ϵ porosity of the accumulated particle cake layer
μ viscosity of solvent (water)
θ porosity dependent variable used in Eq. [5] ($=(1-\epsilon)^{1/3}$)
θ_{max} the value of θ corresponding to maximum random packing of spheres ($\epsilon = 0.36$)

Abbreviations

CP concentration polarization

ACKNOWLEDGMENTS

The authors acknowledge the support of the Center for Environmental Risk Reduction (CERR) at UCLA and the State of California, Department of Water Resources.

REFERENCES

1. Belfort, G., Davis, R. H., and Zydney, A. L., *J. Membr. Sci.* **96,** 1 (1994).
2. Zeman, L. J., and Zydney A. L., ''Microfiltration and Ultrafiltration: Principles and Applications.'' Marcel Dekker, New York, 1996.
3. Song, L., and Elimelech, M., *J. Chem. Soc., Faraday Trans.* **91,** 3389 (1995).
4. Bowen, W. R., and Jenner, F., *Adv. Colloid Interface Sci.* **56,** 141 (1995).
5. Tarleton, E. S., and Wakeman, R. J., *Trans. IChemE* **72,** 431 (1994).
6. Bacchin, P., Aimar, P., and Sanchez, V., *J. Membr. Sci.* **115,** 49 (1996).
7. Cakl, J., and Mikulasek, P., *Sep. Sci. Technol.* **30,** 3663 (1995).
8. Romero, C. A., and Davis, R. H., *Chem. Eng. Sci.* **45,** 13 (1990).
9. Wijmans, J. G., Nakao, S., van den Berg, J. W. A., Troelstra, F. R., and Smolders, C. A., *J. Membr. Sci.* **22,** 117 (1985).
10. Happel, J., *AIChE J.* **4,** 197 (1958).
11. Happel, J., and Brenner, H., ''Low Reynolds Number Hydrodynamics.'' Prentice Hall, Englewood Cliffs, NJ, 1965.
12. Davis, R. H., *Sep. Purif. Methods* **21,** 75 (1992).
13. Fane, A. G., *in* ''Progress in Filtration and Separation'' (R. J. Wakeman, Ed.), Vol. 4, p. 101. Elsevier, Amsterdam, 1986.
14. Israelachvili, J. N., ''Intermolecular and Surface Forces.'' Academic Press, London, 1992.
15. Vigil, G., Xu, Z. H., Steinberg, S., and Israelachvili, J. N., *J. Colloid Interface Sci.* **166,** 367 (1994).
16. Larbot, A., Fabre, J. P., Guizard, C., and Cot, L., *J. Am. Ceram. Soc.* **72,** 257 (1989).
17. Chudacek, M. W., and Fane, A. G, *J. Membr. Sci.* **21,** 145 (1984).
18. Petsev, D. N., Starov, V. M., and Ivanov, I. B., *Colloids Surf. A: Physicochem. Eng. Aspects* **81,** 65 (1993).
19. Bowen, W. R., and Jenner, F., *Chem. Eng. Sci.* **50,** 1707 (1995).